

CONICCURV: A CURVATURE ESTIMATION ALGORITHM FOR PLANAR POLYGONS

[‡]RAFAEL DÍAZ-FUENTES, [‡]JORGE ESTRADA-SARLABOUS, AND [‡]VICTORIA HERNÁNDEZ-MEDEROS

[‡]Department of Mathematics and Computer Science, University of Cagliari, Cagliari, Italy
(rafael.diazfuentes@unica.it)

[‡]Instituto de Cibernética, Matemática y Física, La Habana, Cuba
([jestrada,vicky@icimaf.cu](mailto:{jestrada,vicky}@icimaf.cu)).

ABSTRACT. *ConicCurv* is a new *derivative-free* algorithm to estimate the curvature of a plane curve from a sample of data points. It is based on a known tangent estimator method grounded on classic results of Projective Geometry and Bézier rational conic curves. The curvature values estimated by *ConicCurv* are invariant to Euclidean changes of coordinates and reproduce the exact curvature values if the data are sampled from a conic.

We show that *ConicCurv* has convergence order 3 and, if the sample points are *uniformly arc-length distributed*, the convergence order is 4. The performance of *ConicCurv* is compared with some of the most frequently used algorithms to estimate curvatures and its performance is illustrated in the calculation of the elastic energy of subdivision curves and the location of L-curves corners.

Keywords: curvature estimation, rational conics, geometry processing, L-curves, regularization parameter, *elastica*.

2020 Mathematics Subject Classification: 53Z50, 53A15, 68W25, 65D15, 65F22

1. INTRODUCTION

In several tasks of Computer Aided Geometric Design and Computer Vision it is necessary to estimate curvature values from a sample of few unevenly distributed points [6, 7, 8, 27, 26, 31]. Those values may be used to design curves or surfaces for free design applications, such as typography design, cartoons, and games, among others. The need comes from the interpolation or approximation of a planar set of points with methods that require the estimation of curvature values [5]. Another situation where the data consists of a set of few nonuniform distributed points is found in some Tykhonov regularization problems [9, 11, 23], where the points describe a curve with L-shape or in another cases an U-shape [12, 24]. In these problems, the generation of points on the curves is computationally expensive. When we seek to estimate the location of the points of relative maximum of curvature (corner points) of L-curves or U-curves, it is necessary to locate the desired point with a small sample of points.

The most known curvature estimation methods in the literature use tangent vectors, osculating circles, or first and second order derivatives, depending on the selected curvature definition. In the first case one needs to estimate the derivative of the tangent vector with respect to arc-length. In the second case, the radius of the osculating circle that touches the curve at the desired point is estimated as the radius of the circumference that interpolates that point and two consecutive ones (anterior and posterior neighbors, according to the order of the data). This method offers an intuitive control of the assigned curvature values, but only reproduces the exact curvature values if the data come from a circle, which is a very particular case of the shape that the designer could wish for. In the third case, the estimated values of the first and second derivatives at the point are used to compute the curvature. We refer the interested reader to [6, 22, 26], and references therein, for a fairly complete study of methods to estimate curvature.

The present work introduces *ConicCurv*, a new *derivative-free* algorithm to estimate the curvature of a plane curve from a sample of data points that aims to be consistent with the geometry suggested by the data.

Our proposed method assigns curvature values at each point of an ordered set of data in the plane, calculating the average of the curvatures at the point of two conic curves. Both curves interpolate

the given point as well as the previous and the next neighbors, without computing the equations of these interpolating conics. The first interpolating curve is chosen as the rational conic in Bernstein-Bézier form that, additionally to the three points, interpolates the tangent directions assigned to the previous point and the point in question. Analogously, the second interpolating curve is chosen as the rational conic in Bernstein-Bézier form that, additionally to the three points, interpolates the tangent directions assigned to the point in question and its subsequent neighbor.

If the tangent directions are not provided as data, we estimate them using the tangent estimation method in [1]. In what follows, we refer to this tangent estimation method as ABFH. By coupling ABFH with *ConicCurv* very desirable properties are inherited, such as high convergence order, reproduction of exact curvature values, if the points are sampled from conics, invariance under Euclidean transformations, and local control of the geometry.

In Section 2 we show the preprocessing of the data before curvature estimation. Part of that preprocessing consists on splitting the polygon defined by the data in convex sub-polygons whose vertices are a subset of the original data points in the previously specified order. If there are “many” convexity changes (that is, a considerable number of sub-polygons), the data can be smoothed and then tangents are estimated at each point.

Taking into account the preprocessing of Section 2, in Section 3 curvature values are assigned at each point with a computational cost of $O(n)$, where n is the number of data points, for data preprocessing and curvature estimation with *ConicCurv*. In Section 4 the approximation order of the proposed curvature estimation is shown. In Section 5 the numerical results obtained with *ConicCurv* are compared with those obtained using some methods of curvature estimation reported in the literature [7, 26].

Finally, in Sections 6 and 7 applications of *ConicCurv* to the estimation of the elastic energy of subdivision curves and to the estimation of the location of L-curve corners are reported, respectively.

2. DATA PREPROCESSING

Given an ordered set of points in the plane, in addition to the coordinates of the points, the *ConicCurv* method also requires tangent directions assigned to these points. If the tangent directions are not available *a priori*, the method of assigning tangent directions that we used, as shown in Section 2.1, assumes the convexity of the polygon formed by the data. Therefore, the first step to be carried out in the preprocessing is the splitting of the initial polygon into convex sub-polygons; see Section 2.2. We assume that there are not three consecutive collinear points in the given set. In that case, we set the curvature in the middle point equals to zero and no estimation is performed. This assignment is consistent with the fact that the straight lines are the only irreducible algebraic curves which have an arc that interpolates three collinear points.

As notation, by $\mathcal{P} = \{P_i, i = 1, \dots, n\}$ we refer to an ordered set of points and, at the same time, to the polygon having those n points as vertices in given order. Consequently, $\mathcal{P}(s : r) = \{P_i, i = s, \dots, r\}$, with $1 \leq s \leq r \leq n$, $\mathcal{P}(i) = P_i$, and $|\mathcal{P}| = n$ denotes the cardinality of the set \mathcal{P} .

2.1. Pascal’s theorem and tangent estimation. There are several algorithms for estimating tangent vectors given a set of points in the plane \mathbb{R}^2 . If the polygon that joins pairs of consecutive points in the given order is convex, it is shown that ABFH has an order of approximation 4, higher than other methods in the specialized literature. This tangent estimator algorithm is based on *Pascal’s theorem*.

Theorem 2.1 (Pascal’s theorem). *The three pairs of opposite sides of an hexagon inscribed in a conic section intersect at three collinear points.*

The *principle of duality* of Projective Geometry allows us to express the union of points, that is, the line that joins them, and the intersection of lines by the vector product (also known as exterior or cross product \wedge [17]). It holds that $L_{P_i, P_j} = P_i \wedge P_j$ is the line that passes through the points P_i and P_j , and $L_{P_i, P_j} \wedge L_{P_k, P_l}$ is the intersection point of lines L_{P_i, P_j} and L_{P_k, P_l} . Then, Theorem 2.1 can also be stated in the following way.

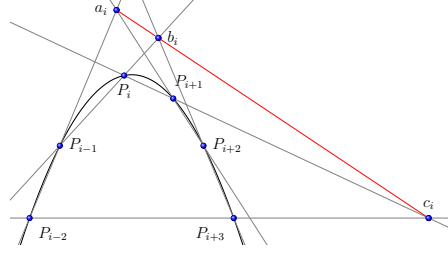


FIGURE 1. Pascal's theorem

Theorem 2.2. Let $P_{i-2}, P_{i-1}, P_i, P_{i+1}, P_{i+2}, P_{i+3}$ be six distinct points in general position, i.e., such that there is no line interpolating three of them, then it holds that the intersection points a_i , b_i , and c_i , defined by

$$a_i = L_{P_{i-2}, P_{i-1}} \wedge L_{P_i, P_{i+1}}, \quad b_i = L_{P_{i-1}, P_i} \wedge L_{P_{i+1}, P_{i+2}}, \quad \text{and} \quad c_i = L_{P_i, P_{i+1}} \wedge L_{P_{i-2}, P_{i+2}},$$

are collinear points; see Fig. 1.

Remark 2.1. Let us note that the point c_i can be computed once a_i and b_i have been obtained, as $c_i = L_{P_{i-2}, P_{i+2}} \wedge L_{a_i, b_i}$. This approach is exploited in the following.

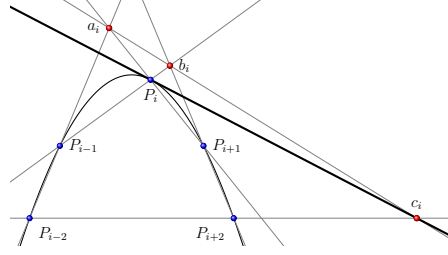


FIGURE 2. Tangent estimation in P_i . This tangent is the limit of the secant $L_{P_i, P_{i+1}}$ in Fig. 1.

In [1] the tangent line of the conic interpolating P_j , $j = i - 2, \dots, i + 2$, at the middle point, P_i , is estimated as a limit case of Pascal's theorem 2.2. When two consecutive points collapse to one point, then the tangent line at this point is the limit of the secant between the two collapsing points; see Fig. 2. Hence, the tangent line r_i at P_i of the conic interpolating $P_{i-2}, P_{i-1}, P_i, P_{i+1}, P_{i+2}$ is $r_i = L_{c_i, P_i}$.

Given the points $\{P_j, j = i - 2, \dots, i + 2\}$, the tangent line at P_i of the conic interpolating those 5 points is computed using Algorithm 1.

Input: $\{P_{i-2}, \dots, P_{i+2}\}$

1: $a_i = L_{P_{i-2}, P_{i-1}} \wedge L_{P_i, P_{i+1}}$

2: $b_i = L_{P_{i-1}, P_i} \wedge L_{P_{i+1}, P_{i+2}}$

3: $c_i = L_{P_{i-2}, P_{i+2}} \wedge L_{a_i, b_i}$

4: $r_i = L_{c_i, P_i}$

Output: r_i

ALGORITHM 1. Tangent line estimation in P_i with the method *ABFH*, proposed in [1].

The tangent lines at the other points can be estimated by changing the ordering.

Remark 2.2. \triangleright The computational cost of Algorithm 1 is 66 flops, since it only requires the computation of the equations of 7 lines joining 2 points and to solve 3 systems of 2 linear equations (the intersection of 3 pairs of such lines).

- ▷ Compared to the method called Conic, which is the method that consists in computing the implicit equation of the conic interpolating the points $\{P_j, j = i-2, \dots, i+2\}$ and calculating from this equation the tangent at one point [1], Algorithm 1 needs fewer computations. The computational cost of Conic is 164 flops, since it requires to solve a system of 5 linear equations and to compute the equation of the tangent line to the conic at P_i .

If we assume that the data P_1, \dots, P_n represent a closed convex polygon, then we estimate the tangent in each point P_i by taking as input for the algorithm the points $P_{i-2}, P_{i-1}, P_i, P_{i+1}, P_{i+2}$, where $P_{-1} = P_{n-1}, P_0 = P_n, P_{n+1} = P_1$, and $P_{n+2} = P_2$. On the other hand, if they represent an open convex polygon, the same procedure is followed except for the extreme points P_1, P_2, P_{n-1} , and P_n . To find r_1 and r_2 , the points P_1, P_2, P_3, P_4, P_5 are reordered so that P_1 and P_2 are, according to the respective case, the third point in the input of the algorithm. Similarly, to find r_{n-1} and r_n , $P_{n-4}, P_{n-3}, P_{n-2}, P_{n-1}, P_n$ are reordered conveniently for each case. In the implementation, it is convenient to work with projective coordinates, so it makes sense to consider the point of intersection even for parallel lines (that intersect at an *improper point*, i.e., a point at *infinity*) and take advantage of the duality in the computation of $r_i \wedge r_j$ (r_i, r_j straight lines) and $P_i \wedge P_j$ (P_i, P_j points), having just one method for both operations.

Since Algorithm 1 is based on finding intersections of lines, it is invariant under affine transformations. By assigning at each point the tangent of the conic that interpolates it together with its 4 closest neighboring points, it can be concluded that the exact tangent directions are recovered if the data are sampled on a conic.

2.2. Convexity analysis of the data. The method of estimating tangents using Algorithm 1 may lead to erroneous results if the polygon $\mathcal{P} = \{P_i, i = 1, \dots, n\}$ is non-convex [1]; see Fig. 3. The solution to this problem is to split \mathcal{P} into convex sub-polygons. In this way, tangents can be estimated independently in each sub-polygon. This splitting can be done by means of two approaches. The *first approach*, proposed in [2], consists in inserting an *inflection point*, P , at the midpoint of the inflection edge $P_i P_{i+1}$, as shown in Fig. 3. Then, the left tangent direction, $\mathbf{t}_{P,l}$, and the right tangent direction, $\mathbf{t}_{P,r}$, at P are estimated associated to the corresponding sub-polygons, that is to say, taking the points $\{P_{i-3}, \dots, P_i, P\}$ and $\{P, P_{i+1}, \dots, P_{i+4}\}$, as entries for Algorithm 1, respectively. Finally, the bisector of the acute angle between them is defined as tangent vector at P ; see Fig. 3. This can be obtained as a convex linear combination of these two tangent vectors.

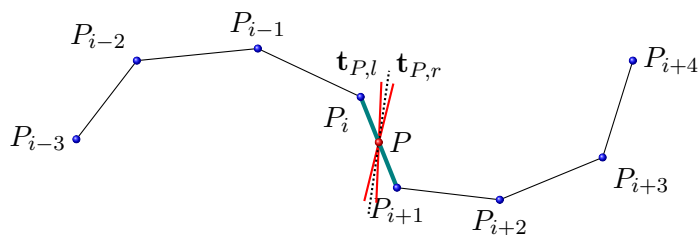


FIGURE 3. Nonconvex polygon divided into two sub-polygon inserting the inflection point P . The assigned tangent is drawn with discontinuous lines.

To avoid inserting more data than the user proposes, a *second approach* consists in dividing the initial polygon into independent convex sub-polygons, considering the inflection edge $\overline{P_i P_{i+1}}$ as belonging to the two sub-polygons that contain it as a final or initial edge, respectively; see Fig. 3. At each point, the tangent is estimated considering only the sub-polygon to which it belongs. Algorithm 2 illustrates the proposal, with $R_{\frac{\pi}{2}}$ denoting a rotation of $\frac{\pi}{2}$ radians, $\langle \cdot, \cdot \rangle$ the usual scalar product, and $sign(x) = \frac{|x|}{x}$ the sign function (discarding the case $x = 0$, as there are not three consecutive collinear points in \mathcal{P}).

<p>Input: $\mathcal{P} = \{P_i, i = 1, \dots, n\}$</p> <p>1: $j = 1;$</p> <p>2: while ($\mathcal{P} \geq 3$) do ▷ The smallest amount of vertices in a sub-polygon is 3.</p> <p>3: $\mathcal{PC}_j(1 : 3) = \mathcal{P}(1 : 3);$</p> <p>4: $s = \text{sign}(\langle P_1 - P_2, R_{\frac{\pi}{2}}(P_3 - P_2) \rangle);$</p> <p>5: $i = 3;$</p> <p>6: $n = \mathcal{P} ;$</p> <p>7: while ($i < n$) and ($\text{sign}(\langle P_{i-1} - P_i, R_{\frac{\pi}{2}}(P_{i+1} - P_i) \rangle) == s$) do</p> <p>8: $\mathcal{PC}_j(i + 1) = \mathcal{P}(i + 1);$</p> <p>9: $i = i + 1;$</p> <p>10: end while</p> <p>11: $\mathcal{P} = \mathcal{P}(i - 1 : n);$</p> <p>12: $j = j + 1;$</p> <p>13: end while</p> <p>Output: $\{\mathcal{PC}_1, \mathcal{PC}_2, \dots, \mathcal{PC}_j\}$</p>

ALGORITHM 2. Splitting the initial polygon \mathcal{P} into convex sub-polygons $\{\mathcal{PC}_j\}$ (second approach).

There are cases in which there is an insufficient amount of input data for the Algorithm 1, that is, there may be sub-polygons with less than 5 vertices. To solve this, in [16] the strategy followed by Albrecht et al. has been generalized, collapsing at a certain point a pair of points (selected in a convenient way) and considering as a straight line joining the points of each pair, a tangent assigned a priori by the designer. This method is also based on finding solutions of systems of 2 linear equations of and does not require the calculation of the implicit equation of the conic.

Only two cases considered in [14] should be additionally considered: when a sub-polygon has 3 or 4 points. The case of 2 points is discarded, because the convexity is analyzed in polygons of at least 3 points. Alternatively, in [2] a way of inserting new points in the polygon is proposed, so that each sub-polygon has at least the 5 points necessary for the estimation of the tangents. This is a rule for automatic point insertion and it is not dependent on the design. It differentiates the cases of 3 and 4 points and ensures that the convexity of the sub-polygon with the new points remains unaffected.

3. CURVATURE COMPUTATION

In this section we show how to efficiently estimate the curvature of a smooth curve \mathbf{c} at a sample of points $\{P_j\}$ using the set $\{r_j\}$ of tangent lines associated to $\{P_j\}$ by ABFH.

Based on a general theorem of E. Cartan [10], which states that two curves are related by a group transformation if and only if their signature curves are identical, in [8] the differential invariant signature curve paradigm was introduced for the invariant recognition of visual objects. In visual applications, a group transformation G (typically either the Euclidean, affine, similarity, or projective group) acts on a space E representing the image space, whose subsets are the objects of interest. A differential invariant I of G is a real-valued function, depending on the curve and its derivatives at a point, which is unaffected by the action of G . Consequently, to construct a numerical approximation to a differential invariant I , that approximation should be computed using appropriate combinations of the coordinates of the sample points. This idea draws a bridge between the discrete and continuous invariant theory. The first example discussed in [8] are the Euclidean plane curves (where the simplest differential invariant of the Euclidean group is the Euclidean curvature) and the 3-points invariant numerical approximations to the Euclidean curvature.

For any three noncollinear points in the plane P_1, P_2 , and P_3 , let us denote by $A[P_1 P_2 P_3]$ the signed area of $\triangle P_1 P_2 P_3$, i.e., $A[P_1 P_2 P_3] = \frac{(P_i - P_j) \wedge (P_i - P_k)}{2}$ (the area is positive if the triangle is traversed in a clockwise direction). The quantity $A[P_1 P_2 P_3]$ is the simplest invariant under the action of the special affine group $SA(2)$ consisting of all area-preserving affine transformations of the plane. According to [30], every joint affine invariant $I(P_1, \dots, P_n)$ depending on the n points P_i is a

function of these triangular areas. It is well known that five points P_0, \dots, P_4 in general position in the plane determine a unique conic section that passes through them. The implicit formula for the 5-points interpolating conic in terms of the invariants $A[P_i P_j P_k]$ is a classical result that may be found in [8, 29]. In a similar way, given three points P_i, P_j, P_k and tangent lines associated to two of them, we can establish the $SA(2)$ -invariant form of the unique conic interpolating these points and the associated tangent directions.

Lemma 3.1. *Let P_i, P_j, P_k be three points in general position in the plane and let r_i, r_k be the tangent lines associated to $P_i, P_k, i \neq k$, respectively. Let $Q = r_i \wedge r_k$. Then, the unique conic \mathcal{C} interpolating P_i, P_j, P_k as well as the tangent directions associated to $P_i, P_k, i \neq k$, satisfies the quadratic $SA(2)$ -invariant implicit equation*

$$A[\mathbf{x}P_iP_k]^2 A[P_jQP_i] A[P_jP_kQ] = A[P_jP_iP_k]^2 A[\mathbf{x}P_kQ] A[\mathbf{x}QP_i], \quad (3.1)$$

where $\mathbf{x} = (x, y)$ is an arbitrary point on \mathcal{C} .

Moreover, if $\triangle P_iP_kQ$ is nondegenerate, the curvature of the unique conic \mathcal{C} at P_i , $\kappa(P_i)$, has the $SE(2)$ -invariant formula

$$\kappa(P_i) = 4 \frac{A[P_iP_kQ] A[P_jP_kQ] A[P_jQP_i]}{A[P_jP_iP_k]^2 \|Q - P_i\|^3}. \quad (3.2)$$

Proof. We write $\mathbf{x} = (x, y)$ and P_j in barycentric coordinates with respect to $\triangle P_iQP_k$,

$$\mathbf{x} = (x, y) = uP_i + vQ + wP_k \quad \text{and} \quad P_j = u_jP_i + v_jQ + w_jP_k,$$

with $u + v + w = u_j + v_j + w_j = 1$. Since $\mathbf{x} = (x, y)$ is an arbitrary point on \mathcal{C} , its barycentric coordinates satisfy the implicit equation

$$v^2 = 4\Omega^2 u w, \quad (3.3)$$

with

$$\Omega^2 = \frac{v_j^2}{4u_j w_j}. \quad (3.4)$$

Recall the geometric interpretation of the barycentric coordinates with respect to $\triangle P_iQP_k$

$$\begin{aligned} u &= \frac{A[\mathbf{x}P_kQ]}{A[P_iP_kQ]}, & v &= \frac{A[\mathbf{x}P_iP_k]}{A[P_iP_kQ]}, & w &= \frac{A[\mathbf{x}QP_i]}{A[P_iP_kQ]}, \\ u_j &= \frac{A[P_jP_kQ]}{A[P_iP_kQ]}, & v_j &= \frac{A[P_jP_iP_k]}{A[P_iP_kQ]}, & \text{and } w_j &= \frac{A[P_jQP_i]}{A[P_iP_kQ]}. \end{aligned} \quad (3.5)$$

Substituting (3.5) in (3.3), we obtain the $SA(2)$ -invariant implicit equation (3.1) of the unique conic \mathcal{C} determined by the 4-points P_i, P_j, P_k and Q .

Given a rational conic \mathcal{C} in Bernstein-Bézier form with control polygon P_i, Q, P_k and parameter Ω , then the well known formula of the curvature of \mathcal{C} at P_i , $\kappa(P_i)$, is [17]

$$\kappa(P_i) = \frac{A[P_iP_kQ]}{\Omega^2 \|Q - P_i\|^3}. \quad (3.6)$$

Substituting the expressions for u_j, v_j and w_j from (3.5) in (3.4), according to (3.6) we obtain the $SE(2)$ -invariant formula (3.2). \square

Given a sample of points $\{P_j\}$ on a smooth curve \mathbf{c} and the set $\{r_j\}$ of tangent lines associated to $\{P_j\}$ by means of ABFH, we denote by $\mathbf{c}_{i-1,r}$ the unique conic interpolating the points $P_j, j = i-1, i, i+1$ and the tangent vectors τ_j at P_j corresponding to $r_j, j = i, i+1$. Analogously, we denote by $\mathbf{c}_{i,l}$ the unique conic interpolating the points $P_j, j = i-1, i, i+1$ and the tangent vectors at $P_j, \tau_j, j = i-1, i$. To each point P_i are associated two auxiliary points $Q_j = r_{j+1} \wedge r_j, j = i-1, i$. According to the previous Lemma 3.1, in order to compute the curvatures at P_i of the interpolating conics $\mathbf{c}_{i,l}$ and $\mathbf{c}_{i-1,r}$ it is only necessary to compute the auxiliary points Q_{i-1}, Q_i , the distances $\|Q_{i-1} - P_i\|, \|Q_i - P_i\|$ and the areas $A[P_{i-1}P_iP_{i+1}], A[P_iP_{i+1}Q_{i-1}], A[P_{i-1}P_{i+1}Q_{i-1}], A[P_{i-1}Q_{i-1}P_i], A[P_iP_{i-1}Q_i], A[P_{i+1}P_{i-1}Q_i], A[P_{i+1}Q_iP_i]$.

Definition 3.1. Let $\kappa_{i,l}(P_i)$ and $\kappa_{i-1,r}(P_i)$ be the curvature values of the interpolating conics $\mathbf{c}_{i,l}$ and $\mathbf{c}_{i-1,r}$ at P_i . Our estimator $\tilde{\kappa}(P_i)$ for the curvature of the curve \mathbf{c} at P_i is defined as

$$\tilde{\kappa}(P_i) = \frac{\kappa_{i,l}(P_i) + \kappa_{i-1,r}(P_i)}{2}. \quad (3.7)$$

Input: $j, \mathcal{P}(j-3, \dots, j+3)$

1: **for** $i = j-1, j, j+1$ **do**

2: $r_i = \text{Algorithm1}(P_{i-2}, \dots, P_{i+2})$;

3: **end for**

4: $Q_{j-1} = r_{j-1} \wedge r_j$;

5: $Q_j = r_j \wedge r_{j+1}$;

6: Compute $A[P_{j-1}P_jP_{j+1}]$;

7: Compute $A[P_jP_{j+1}Q_{j-1}]$, $A[P_{j-1}P_{j+1}Q_{j-1}]$, $A[P_{j-1}Q_{j-1}P_j]$, and $\|Q_{j-1} - P_j\|$;

8: $\kappa_l(P_j) = 4 \frac{A[P_jP_{j+1}Q_{j-1}]A[P_{j-1}P_{j+1}Q_{j-1}]A[P_{j-1}Q_{j-1}P_j]}{A[P_{j-1}P_jP_{j+1}]^2 \|Q_{j-1} - P_j\|^3}$;

9: Compute $A[P_jP_{j+1}Q_j]$, $A[P_{j-1}P_{j+1}Q_j]$, $A[P_{j-1}P_jQ_j]$, and $\|Q_j - P_j\|$;

10: $\kappa_r(P_j) = 4 \frac{A[P_jP_{j+1}Q_j]A[P_{j-1}P_{j+1}Q_j]A[P_{j-1}P_jQ_j]}{A[P_{j-1}P_jP_{j+1}]^2 \|Q_j - P_j\|^3}$;

11: $\tilde{\kappa}(P_j) = \frac{\kappa_l(P_j) + \kappa_r(P_j)}{2}$;

Output: $\tilde{\kappa}(P_j)$

ALGORITHM 3. Curvature estimation $\tilde{\kappa}(P_j)$ with *ConicCurv* method.

The pseudocode in Algorithm 3 is a sketch of an algorithm to estimate curvatures with *ConicCurv*. For any sample of n points, the computational cost of data preprocessing and *ConicCurv* is clearly $O(n)$. In particular, for one run, (i.e., estimating the curvature in the center point of 7 ordered points), the computational cost of Algorithm 3 is 304 flops. An efficient implementation should reuse the intermediate computations of the estimations of tangent lines and curvatures at the previous points obtained with ABFH and *ConicCurv*.

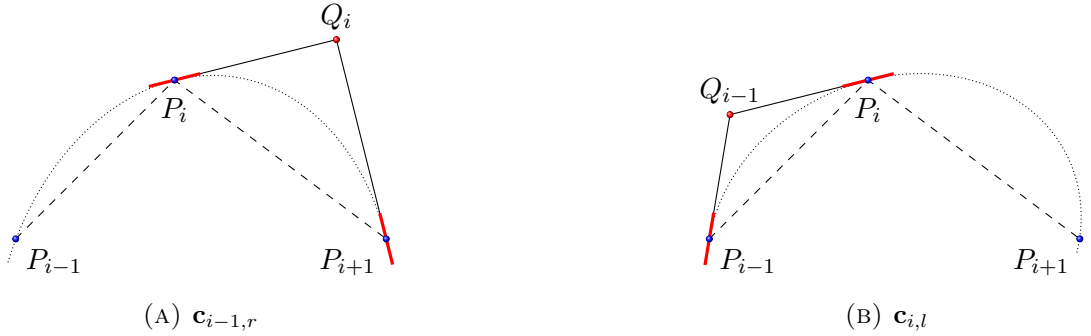


FIGURE 4. Interpolating conics.

4. CURVATURE APPROXIMATION ORDER

Now, we show that, given a discrete sample $\{P_i\}$ of points on a sufficiently differentiable parametric curve $\mathbf{c}(s)$, the average of the curvatures at P_i of the interpolating conics $\mathbf{c}_{i,l}$ and $\mathbf{c}_{i-1,r}$, i.e., $\tilde{\kappa}(P_i)$, provides a good numerical approximation to the curvature of \mathbf{c} at the point P_i .

Let $P_j = \mathbf{c}(s_j)$ and \mathbf{t}_j be the unitary tangent vector of $\mathbf{c}(s)$ at P_j . Our extension of ABFH exposed in Section 2.2 provides vectors τ_j , that are good approximations to \mathbf{t}_j , in the following sense: the tangent vector τ_j corresponding to the tangent line assigned by ABFH to P_j satisfies

$$\tau_j = \mathbf{t}_j + O(h^4) \mathbf{n}_j, \text{ as } h \rightarrow 0, \quad (4.1)$$

where $h = \max_{|k-j| \leq 2} \{|s_k - s_j|\}$ and \mathbf{n}_j is the unitary normal vector of $\mathbf{c}(s)$ at P_j [1].

Theorem 4.1. *Let $\mathbf{c}(s)$ be a parametric curve, C^3 -differentiable in a neighborhood of $P_i = \mathbf{c}(s_i)$ and denote by $\kappa(P_i)$ the curvature of \mathbf{c} at P_i . Then, for $h \rightarrow 0$, the curvature estimator $\tilde{\kappa}(P_i)$ defined by (3.7) satisfies*

$$\kappa(P_i) - \tilde{\kappa}(P_i) = O(h^3).$$

Moreover, if the points P_{i-1} , P_i , and P_{i+1} , are uniformly arc-length distributed, it holds

$$\kappa(P_i) - \tilde{\kappa}(P_i) = O(h^4).$$

Proof. Let be $P_j = \mathbf{c}(s_j)$, $j = 1, 2, \dots$ points on the curve $\mathbf{c}(s)$, \mathbf{t}_j the unitary tangent vectors of $\mathbf{c}(s)$ at P_j , and τ_j the vectors associated to the points P_j by our extension of ABFH exposed in Section 2.2. If $h \max_{|k-j| \leq 2} \{|s_k - s_j|\}$ is very small, for any fixed index i we may assume that for $j \in \{i, i+1\}$ the arc-length from P_{j-1} to P_j on the three curves \mathbf{c} , $\mathbf{c}_{i,l}$ and $\mathbf{c}_{i-1,r}$ are equal; see Fig. 4. Hence, we may arc-length reparametrize \mathbf{c} , $\mathbf{c}_{i,l}$ and $\mathbf{c}_{i-1,r}$, in such a way that it holds

$$\mathbf{c}_{i-1,r}(-s_{i-1}) = \mathbf{c}(-s_{i-1}) = \mathbf{c}_{i,l}(-s_{i-1}) = P_{i-1}, \quad (4.2)$$

$$\mathbf{c}_{i-1,r}(0) = \mathbf{c}(0) = \mathbf{c}_{i,l}(0) = P_i, \quad (4.3)$$

$$\mathbf{c}_{i-1,r}(s_{i+1}) = \mathbf{c}(s_{i+1}) = \mathbf{c}_{i,l}(s_{i+1}) = P_{i+1}, \quad (4.4)$$

where $s_i = 0$.

Recall that for any arc-length parameterized function $\mathbf{r}(s)$, if it is smooth at $s = 0$ and, denoting by $'$ the differentiation with respect to the arc-length s , then $\mathbf{t}(0) = \mathbf{r}'(0)$ and $\mathbf{n}(0) = \mathbf{t}(0)^\perp$ is the Frenet basis at $s = 0$, where \mathbf{v}^\perp denotes the vector orthogonal to vector \mathbf{v} . According to the Frenet formulas it holds

$$\mathbf{r}''(0) = \mathbf{t}'(0) = \kappa(0)\mathbf{n}(0) \quad \text{and} \quad \mathbf{n}'(0) = -\kappa(0)\mathbf{t}(0).$$

Both interpolating conic curves $\mathbf{c}_{i,l}$ and $\mathbf{c}_{i-1,r}$ have the same tangent vector at P_i , τ_i . Therefore, substituting $\mathbf{t}_i = \mathbf{c}'(0)$ in (4.1) we have

$$\mathbf{c}'_{i,l}(0) = \mathbf{c}'_{i-1,r}(0) = \tau_i = \mathbf{c}'(0) + O(h^4)\mathbf{n}_i, \quad \text{as } h \rightarrow 0. \quad (4.5)$$

Moreover, let $\mathbf{n}_{i,l}$ and $\mathbf{n}_{i-1,r}$ be the unit normal vectors of $\mathbf{c}_{i,l}$ (respectively of $\mathbf{c}_{i-1,r}$) at P_i . Since $\mathbf{n}_{i,l} = \mathbf{n}_{i-1,r} = \tau_i^\perp$, from (4.1) it holds

$$\mathbf{n}_{i,l} = \mathbf{n}_{i-1,r} = \mathbf{n}_i + O(h^4)\mathbf{t}_i, \quad \text{as } h \rightarrow 0.$$

Consequently, the principal curvature vectors of the three curves \mathbf{c} , $\mathbf{c}_{i-1,r}$, and $\mathbf{c}_{i,l}$, at P_i are $\mathbf{c}''(0)$, $\mathbf{c}_{i-1,r}''(0)$, and $\mathbf{c}_{i,l}''(0)$, respectively, with

$$\begin{aligned} \mathbf{c}''(0) &= \kappa(P_i)\mathbf{n}_i, \\ \mathbf{c}_{i-1,r}''(0) &= \kappa_{i-1,r}(P_i)\tau_i^\perp = \kappa_{i-1,r}(P_i)\mathbf{n}_i + O(h^4)\mathbf{t}_i, \\ \mathbf{c}_{i,l}''(0) &= \kappa_{i,l}(P_i)\tau_i^\perp = \kappa_{i,l}(P_i)\mathbf{n}_i + O(h^4)\mathbf{t}_i, \end{aligned} \quad (4.6)$$

as h tends to 0, where $\kappa(P_i)$, $\kappa_{i-1,r}(P_i)$, and $\kappa_{i,l}(P_i)$, denote the curvature values at P_i of the curves \mathbf{c} , $\mathbf{c}_{i-1,r}$, and $\mathbf{c}_{i,l}$, respectively.

Expanding $\mathbf{c}(s)$ by its Taylor series around $s = 0$, as s_{i-1} and s_{i+1} tend to 0, we get

$$\mathbf{c}(-s_{i-1}) = \mathbf{c}(0) - s_{i-1}\mathbf{c}'(0) + \frac{s_{i-1}^2}{2}\mathbf{c}''(0) - \frac{s_{i-1}^3}{6}\mathbf{c}'''(0) + O(s_{i-1}^4) \quad (4.7)$$

and

$$\mathbf{c}(s_{i+1}) = \mathbf{c}(0) + s_{i+1}\mathbf{c}'(0) + \frac{s_{i+1}^2}{2}\mathbf{c}''(0) + \frac{s_{i+1}^3}{6}\mathbf{c}'''(0) + O(s_{i+1}^4). \quad (4.8)$$

In a similar way, expanding the interpolating conics by their Taylor series around $s = 0$, as s_{i-1} and s_{i+1} tend to 0, we obtain

$$\begin{aligned} \mathbf{c}_{i-1,r}(-s_{i-1}) &= \mathbf{c}_{i-1,r}(0) - s_{i-1}\mathbf{c}'_{i-1,r}(0) + \frac{s_{i-1}^2}{2}\mathbf{c}''_{i-1,r}(0) - \frac{s_{i-1}^3}{6}\mathbf{c}'''_{i-1,r}(0) \\ &\quad + O(s_{i-1}^4), \end{aligned} \quad (4.9)$$

$$\begin{aligned} \mathbf{c}_{i-1,r}(s_{i+1}) &= \mathbf{c}_{i-1,r}(0) + s_{i+1} \mathbf{c}'_{i-1,r}(0) + \frac{s_{i+1}^2}{2} \mathbf{c}''_{i-1,r}(0) + \frac{s_{i+1}^3}{6} \mathbf{c}'''_{i-1,r}(0) \\ &\quad + O(s_{i+1}^4), \end{aligned} \quad (4.10)$$

$$\mathbf{c}_{i,l}(-s_{i-1}) = \mathbf{c}_{i,l}(0) - s_{i-1} \mathbf{c}'_{i,l}(0) + \frac{s_{i-1}^2}{2} \mathbf{c}''_{i,l}(0) - \frac{s_{i-1}^3}{6} \mathbf{c}'''_{i,l}(0) + O(s_{i-1}^4), \quad (4.11)$$

$$\mathbf{c}_{i,l}(s_{i+1}) = \mathbf{c}_{i,l}(0) + s_{i+1} \mathbf{c}'_{i,l}(0) + \frac{s_{i+1}^2}{2} \mathbf{c}''_{i,l}(0) + \frac{s_{i+1}^3}{6} \mathbf{c}'''_{i,l}(0) + O(s_{i+1}^4). \quad (4.12)$$

From (4.2) we deduce that $2\mathbf{c}(-s_{i-1}) - \mathbf{c}_{i-1,r}(-s_{i-1}) - \mathbf{c}_{i,l}(-s_{i-1}) = 0$, which together with (4.3), (4.5), (4.6), (4.7), (4.9), and (4.11), as h, s_{i-1} , and s_{i+1} tend to 0, leads to

$$\begin{aligned} 0 &= -\frac{s_{i-1}^3}{6} \left(2\mathbf{c}'''(0) - \mathbf{c}'''_{i,l}(0) - \mathbf{c}'''_{i-1,r}(0) \right) + 2s_{i-1}O(h^4)\mathbf{n}_i \\ &\quad + \frac{s_{i-1}^2}{2} (2\kappa(P_i) - \kappa_{i,l}(P_i) - \kappa_{i-1,r}(P_i))\mathbf{n}_i + s_{i-1}^2O(h^4)\mathbf{t}_i + O(s_{i-1}^4). \end{aligned} \quad (4.13)$$

Analogously, with (4.4) on one side showing that $2\mathbf{c}(s_{i+1}) - \mathbf{c}_{i-1,r}(s_{i+1}) - \mathbf{c}_{i,l}(s_{i+1}) = 0$, and substituting on the other side (4.3), (4.5), (4.6), (4.8), (4.10), and (4.12), as h, s_{i-1} , and s_{i+1} tend to 0, we obtain

$$\begin{aligned} 0 &= \frac{s_{i+1}^3}{6} \left(2\mathbf{c}'''(0) - \mathbf{c}'''_{i,l}(0) - \mathbf{c}'''_{i-1,r}(0) \right) - 2s_{i+1}O(h^4)\mathbf{n}_i \\ &\quad + \frac{s_{i+1}^2}{2} (2\kappa(P_i) - \kappa_{i,l}(P_i) - \kappa_{i-1,r}(P_i))\mathbf{n}_i + s_{i+1}^2O(h^4)\mathbf{t}_i + O(s_{i+1}^4). \end{aligned} \quad (4.14)$$

Simplifying the term $\left(2\mathbf{c}'''(0) - \mathbf{c}'''_{i,l}(0) - \mathbf{c}'''_{i-1,r}(0) \right)$ in (4.13) and (4.14), and collecting coefficients of the normal vector we find

$$\frac{2\kappa(P_i) - \kappa_{i,l}(P_i) - \kappa_{i-1,r}(P_i)}{2} = 2\frac{s_{i-1} - s_{i+1}}{s_{i-1}s_{i+1}}O(h^4). \quad (4.15)$$

Being $s_{i-1} = O(h)$ and $s_{i+1} = O(h)$, if $h \rightarrow 0$, it holds

$$\frac{s_{i-1} - s_{i+1}}{s_{i-1}s_{i+1}}O(h^4) = O(h^3). \quad (4.16)$$

Hence, after (4.15) and (4.16) we get

$$\kappa(P_i) - \frac{\kappa_{i,l}(P_i) + \kappa_{i-1,r}(P_i)}{2} = O(h^3), \text{ as } s_{i-1}, s_{i+1} \rightarrow 0.$$

Moreover, if the points $\{P_j, j = i-1, i, i+1\}$ are arc-length uniformly sampled, i.e., $s_{i-1} = s_{i+1}$, from (4.15) and (4.16) it holds

$$\kappa(P_i) - \frac{\kappa_{i,l}(P_i) + \kappa_{i-1,r}(P_i)}{2} = O(h^4), \text{ as } s_{i-1}, s_{i+1} \rightarrow 0.$$

□

Recall that the general 3-points curvature approximations have first order approximation order. In the particular case when the three points are *uniformly* arc-length distributed, the curvature approximation of the general 3-points curvature approximations is of second order [6, 7, 8].

Note that in addition to the third order approximation of the curvature estimator, which is obtained by averaging the curvatures at P_i of the interpolating conics (numerical experiments in the next section show that in fact the approximation order may be very close to $O(h^4)$), this numerical approximation has another advantages. These include invariance with respect to the special Euclidean group of transformations $SE(2)$ and a low computational overhead using the output of ABFH.

5. NUMERICAL EXPERIMENTS

One important objective of the proposed method is to assign curvature values to a set of points, as an intermediate step for free design of curves, where only a small sample of unevenly distributed points are available and small variations in the curvature values do not appreciably affect the shape of the corresponding curve. *ConicCurv* is not supposed to be used to approximate data from image processing or another applications, which are affected by noise or discretization errors. In [22, 26, 31] and in the references contained therein, there is a fairly complete study of the methods to estimate curvature in the case of digital spaces, i.e. curves extracted from images.

5.1. Comparison of curvature estimators. We tested the following four curvature estimation methods by measuring the relative error between the exact curvature value and the corresponding curvature estimates computed on the benchmark of representative curves given in [1] to test tangent estimations. The graph of the curves, the corresponding parametrization and the parametric values of the selected points are shown in Figures 5, 6, 7, 8, 9, 10, 11, and in Table 1.

Let $\mathbf{c}(t)$ be the parametrization of any of the representative curves below. For five parametric values t_j , $j = 1, \dots, 5$ the points $P_j = \mathbf{c}(t_j)$ on $\mathbf{c}(t)$ are computed and, depending on the curvature estimation method, either set of points $\{P_j, j = 2, 3, 4\}$ or $\{P_j, j = 1, 2, 3, 4, 5\}$ is interpolated in order to obtain an estimation of the curvature at point $P_3 = \mathbf{c}(t_3)$.

In our comparison we consider the following curvature estimation methods

- ▷ *Circle*: the estimate of curvature value at P_3 is the inverse of the radius of the circle interpolating $\{P_j, j = 2, 3, 4\}$.
- ▷ *Poly4*: the estimate of curvature value at P_3 is the curvature at P_3 of the fourth degree polynomial curve interpolating $\{P_j, j = 1, 2, 3, 4, 5\}$ at Chebyshev's nodes $\cos\left(\frac{(5-2j)\pi}{10}\right)$, $j = -2, \dots, 2$.
- ▷ *Conic*: the estimate of curvature value at P_3 is the curvature of the conic interpolating $\{P_j, j = 1, 2, 3, 4, 5\}$.
- ▷ *ConicCurv*: the estimate of curvature value at P_3 is the average of the curvature values at P_3 of the conics interpolating the points $\{P_j, j = 2, 3, 4\}$ and the tangent directions assigned by means of ABFH to $\{P_j, j = 2, 3\}$ and to $\{P_j, j = 3, 4\}$, respectively.

The results from the tests are given in Table 2. We can observe that *ConicCurv* shows a better performance than the standard curvature estimation methods in the case of planar convex data.

TABLE 1. Curves tested: curve type, parametrization, and parameter values.

Curve	$\mathbf{c}(t) = (x(t), y(t))$	$(t_1, t_2, t_3, t_4, t_5)$
Polynomial	$\left(t, \frac{1}{5} - \frac{1}{5}(1-t)^5\right)$	(0, 0.1, 0.2, 0.3, 0.4)
Witch of Agnesi	$\left(t, \frac{t}{1+t^2}\right)$	(-2.25, -2, -1.5, -1, -0.75)
Folium of Descartes	$\left(\frac{3t}{t^3+1}, \frac{3t^2}{t^3+1}\right)$	(-0.1, 0.1, 0.3, 0.5, 0.7)
Bicorn	$\left(\sin(t), \frac{\cos^2(t)}{2-\cos(t)}\right)$	(0.139, 0.278, 0.417, 0.556, 0.626)
Tear Drop	$\left(\cos(t), \sin(t) \sin^2\left(\frac{t}{2}\right)\right)$	(1.867, 1.934, 2, 2.034, 2.067)
Exponential	$\left(t, e^{-2(t-0.5)^2}\right)$	(0.2, 0.4, 0.5, 0.8, 0.9)
Ellipse	$(5 \cos(t), 2 \sin(t))$	(0.539, 0.843, 1.222, 1.6, 1.904)

5.2. Approximation order: numerical experiments. The previous numerical experiment shows that using a sample of unevenly distributed points, *Conic* and *ConicCurv* have a substantially better performance compared to another classical curvature estimation schemes.

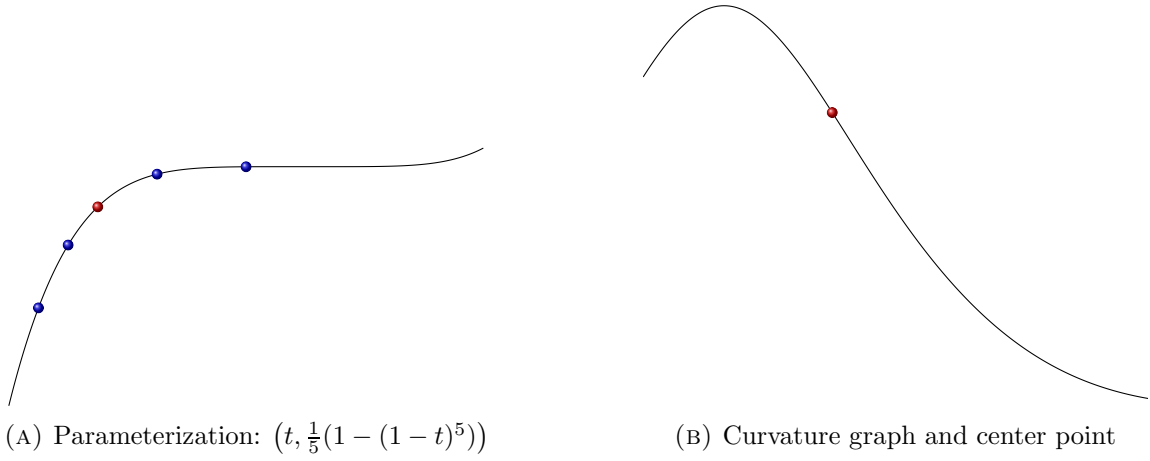


FIGURE 5. Test curve: polynomial.

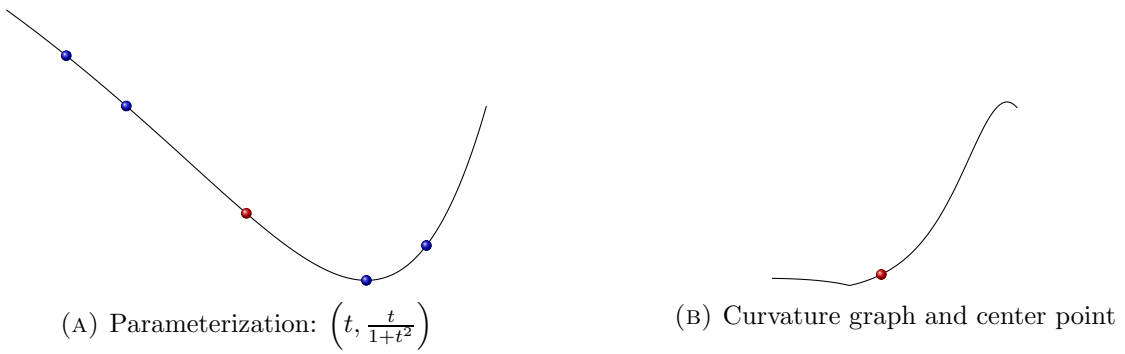


FIGURE 6. Test curve: Witch of Agnesi.

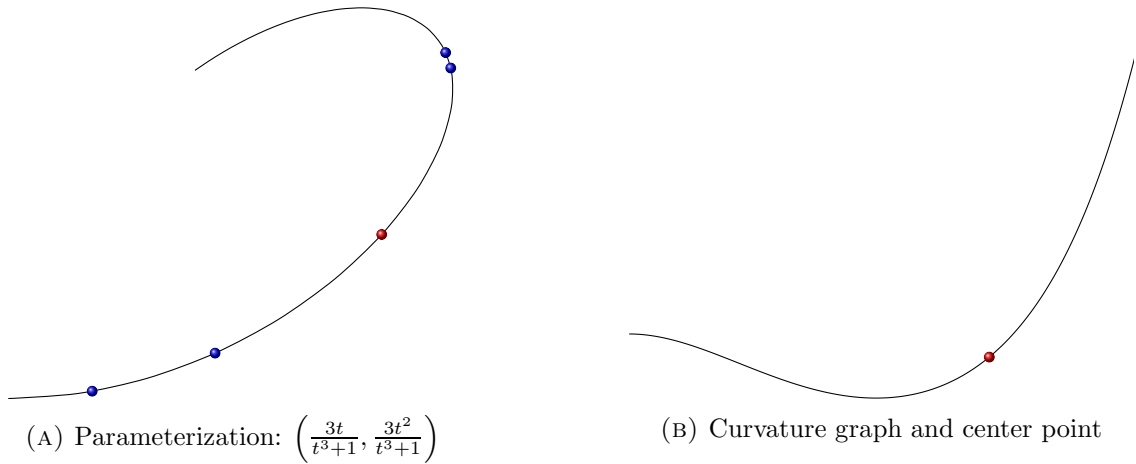


FIGURE 7. Test curve: Folium of Descartes.

The next experiment focuses on the comparison of the approximation order of Conic and *ConicCurv*. Recall that both methods are $SE(2)$ invariant, have *conic precision*, and depend on five data (either 5 points or 3 points and 2 tangent directions).

Let $f : I^k \rightarrow \mathbb{R}$ be the C^3 -continuous function

$$f(t) = \sqrt[4]{1 - t^4}$$

in a neighborhood of $t_3 = 0.7093$ and let $\{h^k = \frac{0.4}{\sqrt{k+2}}, k = 0, 1, 2, \dots, 7\}$ be a strict monotonic decreasing sequence. The exact value of the curvature of $\mathbf{c}(t) = (t, f(t))$ at $P_3 = (t_3, f(t_3)) = (0.7093, 0.9296)$ is $\kappa_{ex} = 1.9199$; see Fig. 12.

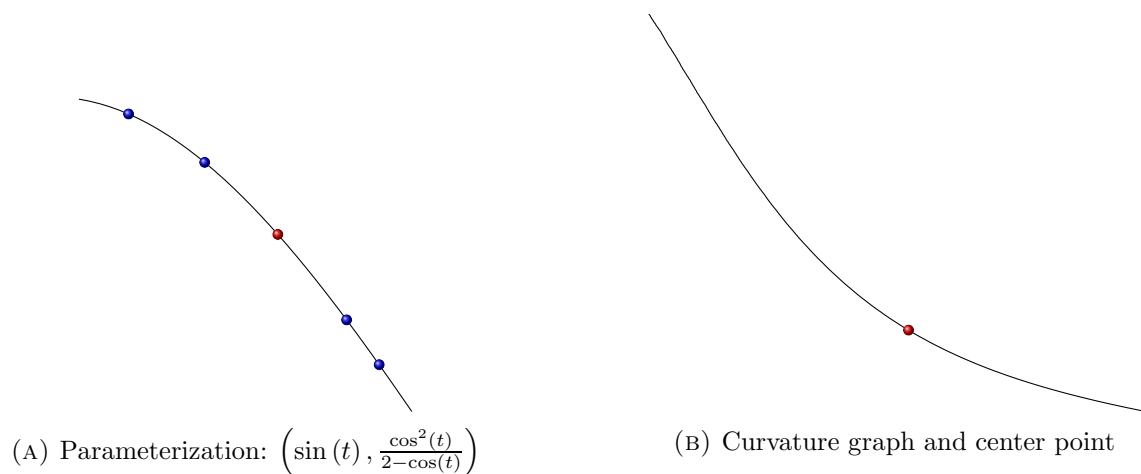


FIGURE 8. Test curve: Bicorn.

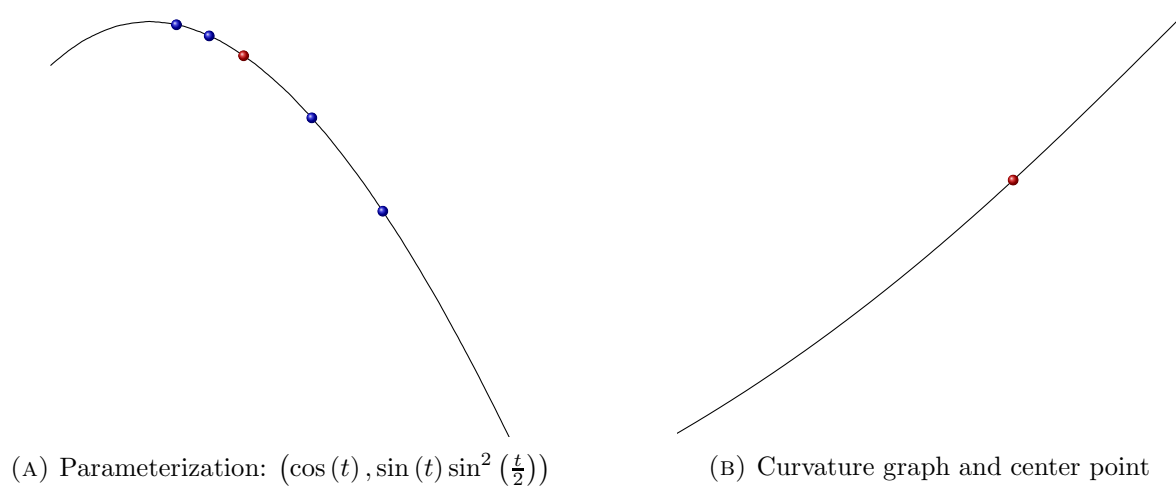


FIGURE 9. Test curve: Tear Drop curve.

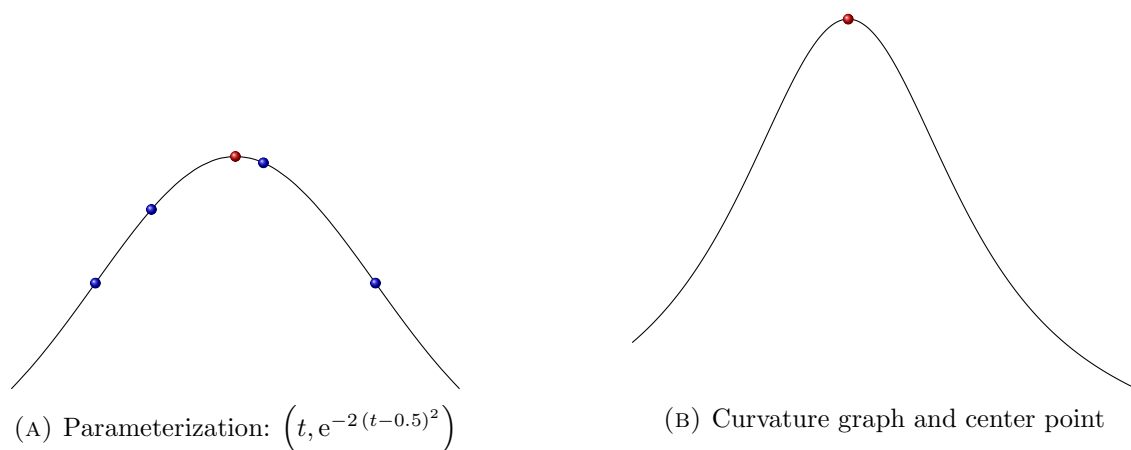


FIGURE 10. Test curve: exponential.

We estimate the approximation order of the curvature values at t_3 obtained with 2 methods, *Conic* and *ConicCurv*, when the values of t_i are selected in the interval

$$I^k = [0.7093 - h^k, 0.7093 + h^k],$$

for $k = 0, 1, 2, \dots, 7$, and $t_3^k = t_3$; see Fig. 13.

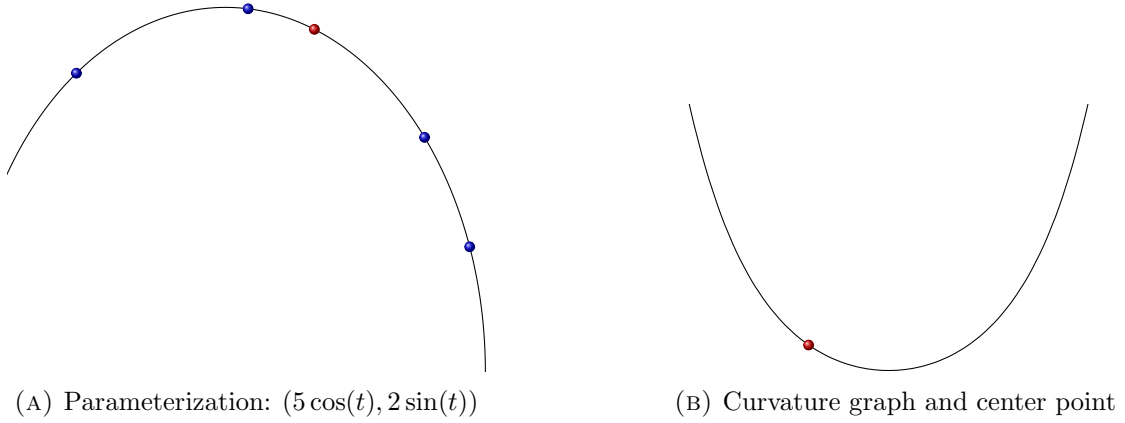


FIGURE 11. Test curve: ellipse.

TABLE 2. Relative error between the exact curvature value for the parameter value t_3 and the corresponding estimates.

Curve	<i>Circle</i>	<i>Poly4</i>	<i>Conic</i>	<i>ConicCurv</i>
Polynomial	0.059	0.123	0.049	0.049
Witch of Agnesi	0.008	0.002	0.007	0.006
Folium of Descartes	0.029	0.110	0.003	0.0001
Bicorn	0.029	0.185	0.006	0.006
Tear Drop	0.030	0.027	0.00008	0.00006
Exponential	0.245	0.790	0.017	0.0006
Ellipse	0.326	0.032	0.000	0.000

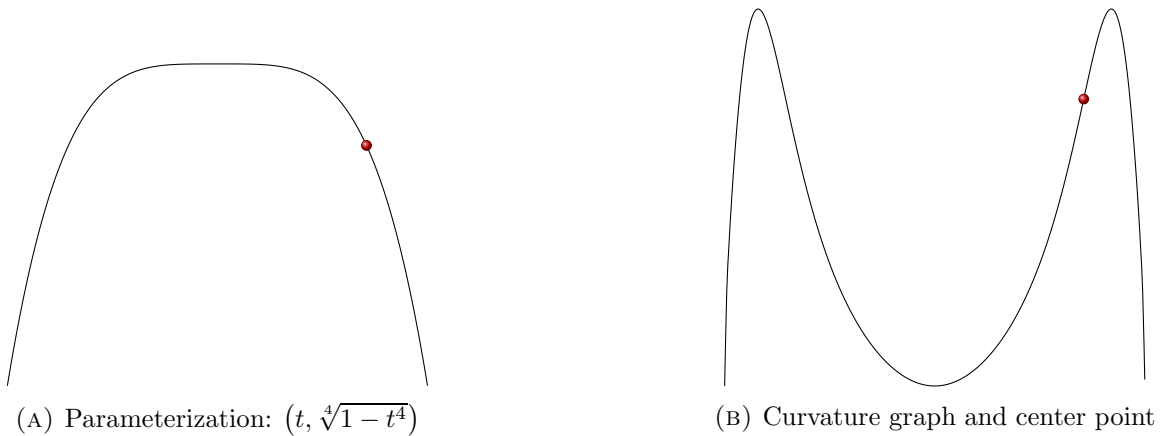


FIGURE 12. Graph of chosen function to compare the methods: Conic and *ConicCurv*.

Conic. For $k = 0, 1, 2, \dots, 7$, it is computed the implicit equation of the conic interpolating the 5 points $\{P_j^k = (t_j^k, f(t_j^k)), j = 1, \dots, 5\}$, with $t_j^k \in I^k$. The condition number of the 5×5 matrix of the linear system of equations whose solution are the coefficients of the implicit equation of the interpolating conic is stored in Cond_k and the relative error between the curvature at t_3^k of the interpolating conic and the exact curvature value is assigned to RE_k .

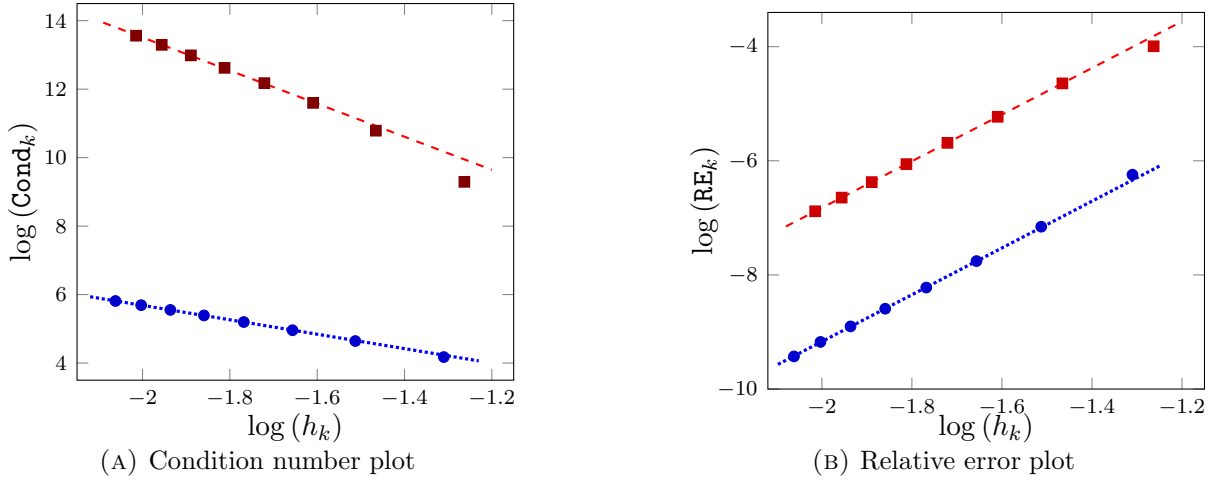


FIGURE 13. Experiments with the methods *Conic* (square red data) and *ConicCurv* (circle blue data). (a) Order of condition number for *Conic* $\approx O(h^{-5})$ and for *ConicCurv* $\approx O(h^{-2})$. (b) Convergence order of *Conic* $\approx O(h^4)$ and for *ConicCurv* $\approx O(h^4)$.

The line fitting the points $(\log(h_k), \log(\text{Cond}_k))$ for $k \geq 2$ has the slope -4.831 , hence the order of the condition number of the 5×5 matrix is close to $O(h^{-5})$; see Figure 13a (red data: square points and dashed lines).

The line fitting the points $(\log(h_k), \log(\text{RE}_k))$ for $k \geq 2$ has the slope 4.084 . Therefore, the approximation order of the curvature estimation with *Conic* is close to $O(h^4)$. See Figure 13b (red data: square points and dashed lines).

ConicCurv. For $k = 0, 1, \dots, 7$, seven points $\{P_j^k = (t_j^k, f(t_j^k)), j = 1, \dots, 7\}$, with $t_j^k \in I^k$ are computed. Tangent lines are assigned to the points $\{P_j^k, j = 2, 3, 4\}$, by means of ABFH applied to the points $P_{j-2}^k, P_{j-1}^k, P_j^k, P_{j+1}^k, P_{j+2}^k$ for $j = 3, 4, 5$, which requires the solution of seven 2×2 linear systems of equations. Then, the auxiliary points $Q_{34}^k = r_3^k \wedge r_4^k$ and $Q_{45}^k = r_4^k \wedge r_5^k$ are computed as the solutions of two 2×2 linear systems of equations. The maximum of the condition numbers of the previous nine 2×2 matrices is assigned to Cond_k .

The line fitting the points $(\log(h_k), \log(\text{Cond}_k))$ for $k \geq 2$ has the slope -2.105 , hence the order of the maximum of the condition numbers of the 2×2 matrices necessary to compute the curvature estimate by means of *ConicCurv* is close to $O(h^{-2})$; see Figure 13a (blue data: circle points and dotted lines).

The estimate of curvature value at P_3 is the average of the curvature values at P_3 of the conics interpolating the points $\{P_j^k, j = 2, 3, 4\}$ and the tangent directions assigned by means of ABFH to $\{P_j^k, j = 2, 3\}$ and to $\{P_j^k, j = 3, 4\}$, respectively. The relative error of the curvature value at P_3 estimated with *ConicCurv* and the exact value is assigned to RE_k .

The line fitting the points $(\log(h_k), \log(\text{RE}_k))$ for $k \geq 2$ has the slope 4.09 . Thus, the approximation order of the curvature estimation with *ConicCurv* is close to $O(h^4)$; see Figure 13b (blue data: circle points and dotted lines).

Remark 5.1. \triangleright In a neighborhood of point P_3 the parametrization $\mathbf{c}(t) = (t, f(t))$ behaves very close to the arc-length parametrization.

- \triangleright The computational overhead and the numerical condition of *Conic* are mainly determined by the solution of the linear system of equations of size 5×5 , that provides the coefficients of the implicit equation of the interpolating conic. The computational overhead and the numerical condition of *ConicCurv* are mainly given by the solution of nine linear systems of equations of size 2×2 .
- \triangleright The relative error of the curvature value at P_3 estimated with *ConicCurv* and the exact value is smaller than the relative error between the curvature at t_3^k of the interpolating conic and the exact curvature value.

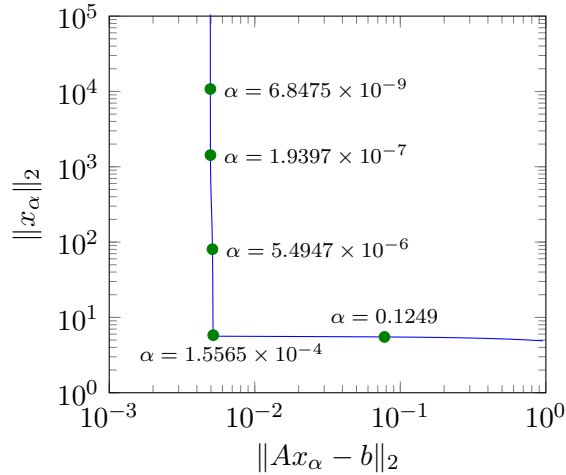


FIGURE 14. Graph of a L -curve and some parametric values.

6. APPLICATION TO CORNER ESTIMATION OF L -CURVES

There are applications where the given set of points has no geometrical meaning for a curve design or a curve approximation, instead they represent data obtained from a particular problem, such as the residual and solution norms of computed solutions dependent on a parameter. The choice of such a parameter is crucial to obtain accurate solutions to ill-posed problems.

Let us consider for instance the linear least-squares problem

$$\min_x \|Ax - b\|_2^2.$$

When the matrix A is ill-conditioned, i.e, its singular values decay rapidly to zero without a significant gap, it is an *ill-posed problem* for which the solution $x = A^\dagger b$ is not stable, where A^\dagger is the Moore-Penrose pseudo-inverse. One of the best-known solution strategies is the Tikhonov regularization, defined by

$$\min_x \|Ax - b\|_2^2 + \alpha^2 \|L(x - x_0)\|_2^2, \tag{6.1}$$

where α is the regularization parameter chosen by the user. The vector x_0 is an *a priori* estimation of the solution. If x_0 is unknown, then it can be set equal the null vector. The regularization (6.1), in its standard form with $L = I$ (identity matrix), reduces to

$$\min_x \|Ax - b\|_2^2 + \alpha^2 \|x\|_2^2. \tag{6.2}$$

There are several strategies to locate the optimal value of the parameter α , one of them is to find the point of maximum curvature (corresponding to the best regularization parameter) of the parametric graph of the norm of the solution versus the corresponding residual norm.

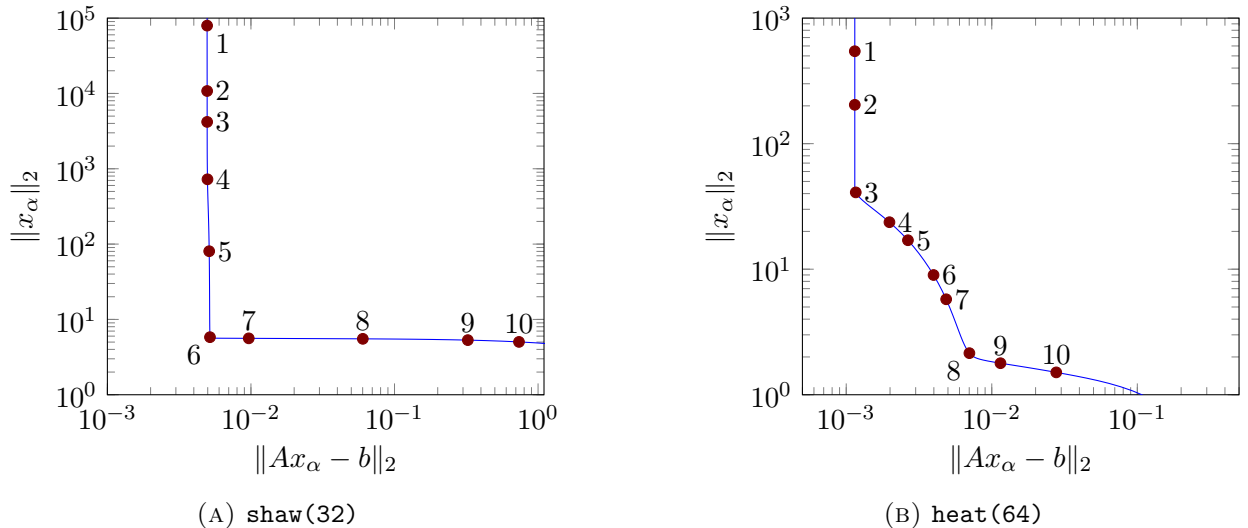
The shape of this curve suggests the letter L (see Fig. 14), therefore, it is called the L -curve. It is customary to process the L -curve in **log-log** scale

$$c(\alpha) = (\log \|Ax_\alpha - b\|_2, \log \|x_\alpha\|_2) \tag{6.3}$$

for the calculation of the optimal parameter [21, 19].

Since the evaluation of points on the L -curve is computationally expensive, it is then preferable to estimate the corner point from a small sample of points on the L -curve. In [9, 11, 23] are proposed algorithms to estimate the location of the corner point of a L -curve. In this context, if *ConicCurv* is applied to assign curvature values to the sample points and to find among them the one corresponding to the maximum curvature, then it happens to be a successful corner point estimation method. Recall that in this case *ConicCurv* furnishes us a *derivative-free* L -curve corner location method, since we do not need to estimate derivatives as in [19].

In order to validate this proposal, numerical experiments are performed with the test problems of the MATLAB package **regutool** (Regularization Tools) [20]. For each problem, several samples of points were selected on the respective L -curve (6.3), considering such points in **log-log** scale. The

FIGURE 15. Sample values to estimate α

obtained results show the reliability of the algorithm based on *ConicCurv* to obtain the point of maximum curvature and thus, the optimal parameter for regularization. For simplicity, only results associated with two test problems are exposed below: **shaw(32)** and **heat(64)**, representatives of problems identified as easy and problematic, respectively [21]. From these two test problems we take the matrix A and the vector b of (6.3), being x_α solution of (6.2).

In fact, for the points shown in Fig. 15a, selected from the L -curve of the problem **shaw(32)** the estimated values are obtained with *ConicCurv* and shown in Table 3. If such estimates are compared with Fig. 15a, the correctness of selecting the point with label 6 as corner point is verified.

In the case of the problem **heat(64)**, considering the points shown in the Table 4 in **log-log** scale and shown in Fig. 15b, the existence of two points with local maximum of curvature (in the respective neighborhoods of the points labeled 3 and 8) can be visually checked.

TABLE 3. Points on the L -curve (**shaw(32)**) and estimated curvature values. The identified corner is highlighted in boldface.

point index	$(\log(\ Ax_\alpha - b\ _2), \log(\ x_\alpha\ _2))$	Estimated curvature values
1	$(-5.3084, 11.2838)$	1.1732×10^{-5}
2	$(-5.3077, 9.2848)$	8.2412×10^{-5}
3	$(-5.3075, 8.3401)$	8.7799×10^{-4}
4	$(-5.3022, 6.5855)$	3.487×10^{-4}
5	$(-5.2748, 4.3874)$	3.9532×10^{-3}
6	$(-5.2621, 1.7596)$	39.773
7	$(-4.6403, 1.7241)$	8.2219
8	$(-2.8107, 1.7089)$	1.2114×10^{-3}
9	$(-1.1266, 1.6699)$	7.8662×10^{-4}
10	$(-0.3058, 1.6152)$	1.0444×10^{-5}

For the chosen data, it can be seen in Table 4 that the local curvature extremes are correctly detected and that point 8 may be considered a global extreme.

As mentioned in Section 2, in order to estimate tangent directions on the data (using Algorithm 1), each convex sub-polygon must have at least 5 points. In this specific application, it is not necessary

TABLE 4. Points on the L -curve (**heat(64)**) and curvature values estimated. The identified corner is highlighted in boldface.

point index	$(\log(\ Ax_\alpha - b\ _2), \log(\ x_\alpha\ _2))$	Estimated curvature values
1	(-6.7722, 6.3001)	2×10^{-4}
2	(-6.7722, 4.0542)	7.56×10^{-2}
3	(-6.7569, 3.7114)	28.51
4	(-6.2239, 3.1644)	4.256×10^{-1}
5	(-5.9314, 2.8339)	1.877×10^{-1}
6	(-5.5260, 2.1960)	1.786×10^{-1}
7	(-5.3267, 1.7511)	3.49×10^{-2}
8	(-4.9590, 0.7627)	153.4
9	(-4.4674, 0.5786)	2.812×10^{-1}
10	(-3.5849, 0.4102)	6×10^{-3}

to use any of the two variants presented above, which are based on inserting new points (see [2]) or tangent directions (see [16]) if necessary. Instead, the necessary additional points can be generated on each sub-polygon by varying the regularization parameter and finding few new points on the L -curve.

The authors believe that the curvature estimation method ConicCurv may be advantageously combined with the algorithm *discrete L-curve criterion* in [21]. Let us use the same notations of Adaptive Pruning Algorithm in [21]. If for each pruned L -curve with \hat{p} points (assumed to be convex) we compute with the aid of ConicCurv estimates of the tangent lines and curvatures at the \hat{p} points of the pruned L -curve, then we may locate the corner by comparing the curvatures estimated with ConicCurv (observe that the slopes ϕ_j in [21] associated to the candidates of corner points are already computed as intermediate result of applying ConicCurv to each pruned L -curve, i.e., the tangent vectors τ_j obtained from ABFH method). Certainly, considering the curvature estimates obtained with ConicCurv instead of the angle between subsequent line segments of the pruned L -curve is a more robust and accurate approach, especially in the case of non-uniform arc-length distributed points.

Compared to the algorithmic discrete L -curve criterion, the combination of ConicCurv and the algorithmic discrete L -curve criterion is more computationally expensive, but the computational cost remains in both approaches of the same order, since estimating tangent lines and curvatures at the \hat{p} points for each pruned L -curve is of order $O(\hat{p})$.

7. APPLICATION TO SUBDIVISION SNAKES

A very popular technique in curve design and Computer Vision is to construct a spline curve that interpolates a sequence of points on the plane. There are infinitely many smooth curves that satisfy these interpolation conditions, so it is desirable to select the one that *best fits* the data. In the context of image segmentation, a popular approach is to start with an initial user-provided curve configuration that automatically deforms itself to delineate the boundary of the object of interest. The deformation is driven by the minimization of an energy functional [3]. In this sense, it is introduced the notion of *elastica*, which is the curve that minimizes a certain functional from the Theory of Elasticity [25]. This functional depends on the coordinates of the points, and some magnitudes that typically are computed from the curve and its derivatives, such as tangent vectors, arc lengths and curvatures.

The present work may be included in a recent trend for curve and surface subdivision schemes, that consists in taking advantage of the hierarchical nature of subdivision schemes (allowing to generate increasingly dense samples of points on the limit spline curve) to propose algorithms for

the computation of energy functionals; see, for instance, [3, 4, 13, 15]. In this section, we show that it is possible to efficiently compute *elastica* with interpolatory subdivision snakes.

For the sake of simplicity, we sketch how to compute approximations of the functional $E + \lambda S$, where $E = \int_0^L \kappa^2(s) ds$ and $S = \int_0^L ds$, for a smooth curve arc length parameterized, with total arc length L . This linear combination of the bending energy E and stretching energy S happens to be a popular energy functional in computer vision and image segmentation.

Given an initial control polygon $\mathcal{P} = \{P_i \in \mathbb{R}^d, i = 1, \dots, n\}$, we can generate a sequence of polygons by doubling their amount of points in each iteration but preserving the points already defined. In such a setting, a binary interpolatory subdivision scheme $\mathcal{F} : \mathcal{P}^j \rightarrow \mathcal{P}^{j+1}$ is a rule that generates recursively polygons $\mathcal{P}^{j+1} = \mathcal{F}(\mathcal{P}^j) = \{P_i^{j+1}, i = 1, \dots, 2^{j+1}n\}$ that refine the previous ones. For instance, we can consider a two-point interpolatory subdivision scheme:

$$\begin{cases} P_{2i-1}^{j+1} = P_i^j \\ P_{2i}^{j+1} = F(P_{i-1}^j, P_i^j), \end{cases}$$

for certain $F : \mathbb{R}^d \times \mathbb{R}^d \rightarrow \mathbb{R}^d$ and initial condition $\mathcal{P}^0 = \{P_i^0 = P_i, i = 1, \dots, n\}$. For a suitable choice of F the sequence of polygons converges uniformly to a smooth curve, the so-called *limit curve* [28]. In general, a boundary rule have to be proposed (for $i = 2^j n$); however, in the context of our use, we just discard that last point and $|\mathcal{P}^{j+1}| = 2|\mathcal{P}^j| - 1$.

Without loss of generality, we may restrict the presentation to the approximation of E and S for a convex arc of the limit curve with endpoints P_{i-1}^0 and P_{i+1}^0 . Given $j \geq 1$, iterating j -times the subdivision scheme \mathcal{F} with initial polygon $\mathcal{P}^0 = \{P_{i-1}^0, P_i^0, P_{i+1}^0\}$ a refined polygon $\mathcal{P}^j = \{P_m^j, m = 2^j(i-1), \dots, 2^j(i+1)\}$ is obtained.

The $2^{j+1} - 1$ chords $P_m^j P_{m+2}^j$, $m = 2^j(i-1), \dots, 2^j(i+1) - 2$, have their end points on the arc of the limit curve. Then, the length of the curve section (stretching energy) can be approximated by the sum

$$S_j = \sum_{r=0}^{2^j-1} \Delta_{2^j(i-1)+2r}^j \quad \text{with} \quad \Delta_m^j = \|P_{m+2}^j - P_m^j\|. \quad (7.1)$$

On the other hand, the mid point quadrature formula provides an approximation to the bending energy

$$E_j = \sum_{r=0}^{2^{j-1}-1} \kappa \left(P_{2^j(i-1)+2r+1}^j \right)^2 \Delta_{2^j(i-1)+2r}^j, \quad (7.2)$$

where $\kappa(\cdot)$ denotes the curvature at the specified point.

Recalling that $P_m^j = P_{4m}^{j+2}$, if $2^{j+2}(i-1) + 3 \leq 4m \leq 2^{j+2}(i+1) - 3$ holds, then the set of 7 consecutive points $\mathcal{C}_m^j = \{P_l^{j+2}, l = 4m-3, \dots, 4m+3\}$ is contained in \mathcal{P}^{j+2} and we may compute an approximation to the curvature at point P_m^j , i.e., $\tilde{\kappa}(P_m^j)$ by applying Algorithm 3 to \mathcal{C}_m^j . It is straightforward to check that if $m = 2^j(i-1) + 2r + 1$ with $r = 0, 1, \dots, 2^{j-1} - 1$, then it holds $2^{j+2}(i-1) + 3 \leq 4m \leq 2^{j+2}(i+1) - 3$. Hence the bending energy (7.2) may be approximated by the formula

$$\tilde{E}_j = \sum_{r=0}^{2^{j-1}-1} \left(\tilde{\kappa}(P_{2^{j+2}(i-1)+8r+4}^{j+2}) \right)^2 \Delta_{2^j(i-1)+2r}^j,$$

where $\tilde{\kappa}(P_{2^{j+2}(i-1)+8r+4}^{j+2})$ denotes the curvature at $P_{2^j(i-1)+2r+1}^j = P_{2^{j+2}(i-1)+8r+4}^{j+2}$ estimated by applying Algorithm 3 to $\mathcal{C}_{2^j(i-1)+2r+1}^j$.

Let $j^* > 1$ be a fixed maximum number of iterations of the subdivision scheme \mathcal{F} . Without much computational effort, we can achieve estimations of the energy functionals S and E with the accuracy required by Computer Design and Computer Vision applications for relatively small values of j^* . For fixed j^* (usually with j^* equals 4 or 5) sufficiently accurate estimations are obtained. For those applications requiring estimates of high order of accuracy, the remarkable effective procedure

called Richardson extrapolation may be used; see [18]. The pseudocode in Algorithm 4 shows a very simplified algorithm for a *derivative-free* estimation of the elastic energies (7.1) and (7.2).

Input: $j^*, \mathcal{P}^0 = \{P_{i-1}, P_i, P_{i+1}\}$

```

1: for  $j = 1, \dots, j^*$  do
2:    $\mathcal{P}^j = \mathcal{F}(\mathcal{P}^{j-1});$ 
3: end for
4:  $S = 0;$ 
5: for  $r = 0, \dots, 2^{j^*} - 1$  do
6:    $m = 2^{j^*}(i-1) + 2r;$ 
7:    $\Delta_m^{j^*} = \|P_{m+2}^{j^*} - P_m^{j^*}\|$ 
8:    $S = S + \Delta_m^{j^*};$ 
9: end for
10:  $E = 0;$ 
11: for  $h = 1, \dots, 2^{j^*-1} - 1$  do
12:    $\delta_h^{j^*-2} = \sum_{r=4(h-1)}^{4h-1} \Delta_{2^{j^*}(i-1)+2r}^{j^*};$ 
13:    $m = 2^{j^*}(i-1) + 2h;$ 
14:    $\kappa_h^{j^*} = \tilde{\kappa}(P_m^{j^*}) = \text{Algorithm 3}(P_{m-3}^{j^*}, \dots, P_{m+3}^{j^*});$ 
15:    $E = E + (\kappa_h^{j^*})^2 \delta_h^{j^*-2};$ 
16: end for
Output:  $S, E$ 

```

ALGORITHM 4. Stretch and bending energy estimation with *ConicCurv* method.

The computational cost of applying Algorithm 4 with bounded j^* to the subdivision curve arc with initial control polygon $\{P_{i-1}, P_i, P_{i+1}\}$ is $O(1)$. Hence, if applied to a control polygon with n vertices, the computational cost is $O(n)$.

The following numerical experiment illustrates the performance of *ConicCurv* to estimate the stretch and bending energy of an ellipse arc by generating increasingly dense samples of points with the binary interpolating subdivision scheme presented in [4, 14]. Consider the ellipse from the benchmark of representative curves given in Table 1. Let be $P_{i-1}^0 = (2.7015, 1.6829)$, $P_i^0 = (0.3536, 1.994)$, $P_{i+1}^0 = (-2.0807, 1.8185)$ points on the ellipse, the Table 5 shows the relative errors of the estimations of stretch and bending energy for the ellipse arc with end points P_{i-1}^0 and P_{i+1}^0 , applying *Algorithm 4* with $j^* = 2, 3, 4$.

TABLE 5. Relative errors of energies S and E estimated with *ConicCurv* for increasing maximum number of iterations j^* .

j^*	Error of estimated S	Error of estimated B
2	0.0071	0.2057
3	0.0018	0.0665
4	0.0004	0.0089

8. CONCLUSIONS

We have presented *ConicCurv*, a new *derivative-free* and $SE(2)$ -invariant algorithm to estimate the curvature of a plane curve from a sample of data points. This algorithm has *conic precision* and is based on a known method to estimate tangent directions, that is grounded on classic results of Projective Geometry and Bézier rational conic curves.

Our theoretical study corroborates the results of the presented numerical experiments: in convex settings *ConicCurv* has approximation order 3, while classical 3-*points* curvature approximations that are invariant with respect to the special Euclidean group of transformations have approximation order 1. Further, if the sample points are *uniformly arc-length distributed*, the approximation order is 4.

The performances of *ConicCurv* were shown by comparing it with some of the most frequently used algorithms to estimate curvatures. Finally, its effectiveness was illustrated as a *derivative-free* estimator of the elastic energy of subdivision curves and of the location of L-curve corners. An open source implementation is available at <https://github.com/RafaelDieF/ConicCurv>.

As a completion of the previous researches, a future direction can be pointed out: to extend the curvature estimation method to data on a curve in the space \mathbb{E}^3 ; see [13, 27].

ACKNOWLEDGMENTS

R.D.F. is member of the Gruppo Nazionale per l'Analisi Matematica, la Probabilità e le loro Applicazioni (GNAMPA) of the Istituto Nazionale di Alta Matematica (INdAM) and acknowledges financial support by PNRR e.INS Ecosystem of Innovation for Next Generation Sardinia (CUP F53C22000430001, codice MUR ECS0000038).

REFERENCES

- [1] G. Albrecht, J.-P. Bécar, G. Farin, and D. Hansford. On the approximation order of tangent estimators. *Computer Aided Geometric Design*, 25(2):80–95, 2 2008.
- [2] G. Albrecht and L. Romani. Convexity preserving interpolatory subdivision with conic precision. *Applied Mathematics and Computation*, pages 4049–4066, 2012.
- [3] A. Badoual, D. Schmitter, V. Uhlmann, and M. Unser. Multiresolution subdivision snakes. *IEEE Transactions on Image Processing*, 26(3):1188–1201, 3 2017.
- [4] L. Barrera Rodríguez, J. Estrada Sarlabous, S. Behar Jequín, and S. Leyva Sánchez. Implementation of a fair Hermite interpolatory scheme based on quadratic A-spline elastica. *Revista Investigación Operacional*, 44(4):516–523, 2023.
- [5] S. Behar-Jequín, J. Estrada-Sarlabous, and V. Hernández-Mederos. Constrained interpolation with implicit plane cubic a-splines. In José Ruiz-Shulcloper and Walter G. Kropatsch, editors, *Progress in Pattern Recognition, Image Analysis and Applications*, pages 724–732, Berlin, Heidelberg, 2008. Springer Berlin Heidelberg.
- [6] A. Belyaev. Plane and space curves. curvature. curvature-based features. <http://www.mpi-sb.mpg.de/~belyaev/gm06>
- [7] A. Belyaev. A note on invariant three-point curvature approximations. *Surikaiseikikenkyusho Kokyuroko (RIMS Kyoto)*, 1111:157–164, 1999.
- [8] E. Calabi, P.J. Olver, C. Shakiban, A. Tannenbaum, and S. Haker. Differential and numerically invariant signature curves applied to object recognition. *International Journal of Computer Vision*, 26:107–135, 1998.
- [9] D. Calvetti, S. Morigi, L. Reichel, and F. Sgallari. Tikhonov regularization and the L-curve for large discrete ill-posed problems. *Journal of Computational and Applied Mathematics*, 123(1):423–446, 2000. Numerical Analysis 2000. Vol. III: Linear Algebra.
- [10] É. Cartan. La méthode du repère mobile, la théorie des groupes continus, et les espaces généralisés. Exposés de géométrie V, 1935.
- [11] J.L. Castellanos, S. Gómez, and V. Guerra. The triangle method for finding the corner of the L-curve. *Applied Numerical Mathematics*, 43(4):359–373, 2002.
- [12] M. Chen, H. Su, Y. Zhou, C. Cai, D. Zhang, and J. Luo. Automatic selection of regularization parameters for dynamic fluorescence molecular tomography: a comparison of l-curve and u-curve methods. *Biomedical Optics Express*, 7(12):5021–5041, Dec 2016.
- [13] R. Díaz Fuentes. *Solving the Hermite interpolation problem with scalar subdivision schemes*. PhD thesis, Università degli Studi dell'Insubria, Italia, 2021.
- [14] R. Díaz Fuentes and J. Estrada Sarlabous. Algoritmo de asignación de curvatura para datos en el plano. Technical Report 721, ICIMAF, November 2013.
- [15] R. Díaz Fuentes, J. Pino Torres, V. Hernández Mederos, and J. Estrada Sarlabous. Stationary Subdivision Snakes for Contour Detection. *Revista Investigación Operacional.*, 42(2):238–266, 2021.
- [16] J. Estrada Sarlabous and R. Díaz Fuentes. Esquema de subdivisión interpolatorio basado en spline cónico. Technical Report 582, ICIMAF, November 2010.
- [17] G Farin. *Curves and surfaces for CAGD: a practical guide*. Morgan Kaufman Publishers Inc., 5 edition, 2002.
- [18] M. Floater, A. Rasmussen, and U. Reif. Extrapolation methods for approximating arc length and surface area. *Numerical Algorithms*, 44:235–248, 2007.
- [19] P. C. Hansen and D. P. O'Leary. The use of the L-curve in the regularization of discrete ill-posed problems. *SIAM Journal on Scientific Computing*, 14:1487–1503, 1993.

- [20] P.C. Hansen. Regularization tools version 4.0 for matlab 7.3. *Numerical Algorithms*, 46(2):189–194, 2007.
- [21] P.C. Hansen, T.K. Jensen, and G. Rodriguez. An adaptive pruning algorithm for the discrete L-curve criterion. *Journal of Computational and Applied Mathematics*, 198(2):483–492, 2007.
- [22] S. Hermann and R. Klette. A Comparative Study on 2D Curvature Estimators. In *International Conference on Computing: Theory and Applications (ICCTA '07)*, pages 584–589, Kolkata, India, 2007.
- [23] S. Kindermann and K. Raik. A simplified L-curve method as error estimator. *ETNA - Electronic Transactions on Numerical Analysis*, 53:217–238, 2019.
- [24] D. Krawczyk-Stańdo and M. Rudnicki. Regularization parameter selection in discrete ill-posed problems - the use of the U-curve. *International Journal of Applied Mathematics and Computer Science*, 17(2):157–164, 2007.
- [25] L. Landau and E. Lifshitz. *Theory of Elasticity*. London, U.K, 1959.
- [26] T. Lewiner, J. Gomes, H. Lopes, and M. Craizer. Arc-length based curvature estimator. *Sibgrapi 2004 (XVII Brazilian Symposium on Computer Graphics and Image Processing)*, pages 250–257, 2004.
- [27] J. Peng, Q. Li, C.-C. J. Kuo, and M. Zhou. Estimating gaussian curvatures from 3D meshes. In *Human Vision and Electronic Imaging VIII*, volume 5007 of *SPIE Proceedings*, pages 270–280. SPIE, 2003.
- [28] M. Sabin. *Analysis and Design of Univariate Subdivision Schemes*. Springer, 2010.
- [29] B. Sturmfels. *Algorithms in Invariant Theory*. Springer-Verlag, New York, 1993.
- [30] H. Weyl. *Classical Groups*. Princeton, N.J., 1946.
- [31] M. Worring and A.W.M. Smeulders. Digital curvature estimation. *CVGIP: Image Understanding*, 58(3):366–382, 1993.